Optics and Laser Technology 122 (2020) 105860

Contents lists available at ScienceDirect

Optics and Laser Technology

journal homepage: www.elsevier.com/locate/optlastec

Full length article

Self-Q-switching and passively Q-switched mode-locking of dual-wavelength Nd:YSAG laser

Congcong Gao[a], Shuhui Lv[a], Guo Zhu[a], Guoju Wang[a], Xiancui Su[a], Beibei Wang[a], Santosh Kumar[a], Renqin Dou[b], Fang Peng[b], Qingli Zhang[b], Haijuan Yu[c], Xuechun Lin[c], Bingyuan Zhang[a,*]

[a] Shandong Key Laboratory of Optical Communication Science and Technology, School of Physics Science and Information Technology, Liaocheng University, Liaocheng 252059, China
[b] The Key Laboratory of Photonic Devices and Materials of Anhui, Anhui Institute of Optics and Fine Mechanics, Chinese Academy of Sciences, Hefei 230031, China
[c] Institute of Semiconductors, Chinese Academy of Sciences, Beijing 100083, China

HIGHLIGHTS

- The performance of self-Q-switching Nd:YSAG operation is studied.
- A stable black phosphorus saturable absorber (BP-SA) was prepared.
- The passively Q-switched mode-locking operation by using BP-SA is investigated.
- Generation of dual-wavelength picosecond pulses by QML operation.
- SQS and QML operating at dual-wavelengths of 1058.97 and 1061.49 nm, respectively.

ARTICLE INFO

Keywords:
Self-Q-switched
Passively Q-switched mode-locked
Dual-wavelength
Black phosphorus saturable absorber

ABSTRACT

In this paper, self-Q-switched (SQS) and passively Q-switched mode-locked (QML) dual-wavelength Nd:YSAG lasers are reported, that works at 1058.97 and 1061.49 nm, simultaneously. Till now, the performance on SQS, and passively QML operation by using black phosphorus (BP) in Nd:YSAG crystal lasers have not been reported as per the author's knowledge. The Nd:YSAG laser SQS operation was realized by designing a simple plano-plano resonator cavity. The maximum output power of 0.471 W at absorbed pump power 2.64 W and the pulse duration was 885 ns. The Nd:YSAG laser QML operation was realized by designing a Z-type resonator cavity. The duration of mode-locked pulse inside the Q-switched envelop was estimated to be 235 ps with 96.5 MHz repetition rate at the absorbed pump power of 4.08 W in QML with black phosphorus saturable absorber (BP-SA).

1. Introduction

Dual-wavelength lasers are widely used in optical communication, spectral analysis, environmental monitoring, and especially terahertz (THz) frequency generation. It has exceptional capability of dual-wavelength ultrafast lasers of producing pulse trains at different center wavelengths [1–4]. Till now, many dual-wavelength lasers using Nd-doped crystals, such as Nd:GGG [5], Nd:$GdVO_4$ [6], Nd:YVO_4 [7], Nd:YAG [8], Nd:LuAG [9] have been reported. Among these crystals, Nd:YAG is mostly used laser material because of its low threshold, high efficiency, excellent thermal, and mechanical properties [10]. However, the radiation resistance of the Nd:YAG is very poor that affects its application in space laser. In addition, the laser efficiency reduces with doping of the external Nd^{3+}-ion. The fluorescence spectrum also changes to narrow, so it is difficult to realize the picosecond laser output. To eliminate the above-mentioned bottleneck, Lutts et al. [11] developed the Nd:YSAG garnet crystal using Czochralski and floating zone melting method. In that, lattice and quenching of Nd^{3+}-ion concentration were alleviated by partially replacing the $A1^{3+}$-ion with Sc^{3+}-ion in YAG crystal that results in a larger ionic radius [12]. In addition, the disorder of the YSAG lattice results in an inhomogeneous broadening of the absorption and emission bandwidth of Nd:YSAG due to the random substitution of $A1^{3+}$-ion [12]. Therefore, it possesses a significantly prolonged fluorescence lifetime. Means, the Nd:YSAG

* Corresponding author.
E-mail address: bingyuanzhang@yahoo.com (B. Zhang).

https://doi.org/10.1016/j.optlastec.2019.105860
Received 25 June 2019; Received in revised form 16 August 2019; Accepted 17 September 2019
Available online 24 September 2019
0030-3992/

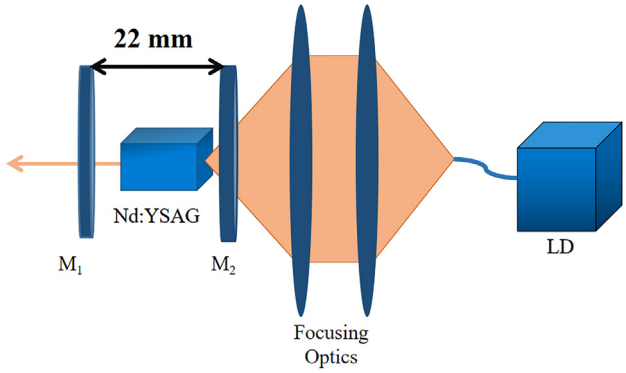

Fig. 1. Experimental setup of the Nd:YSAG continuous wave and self-Q-switched laser.

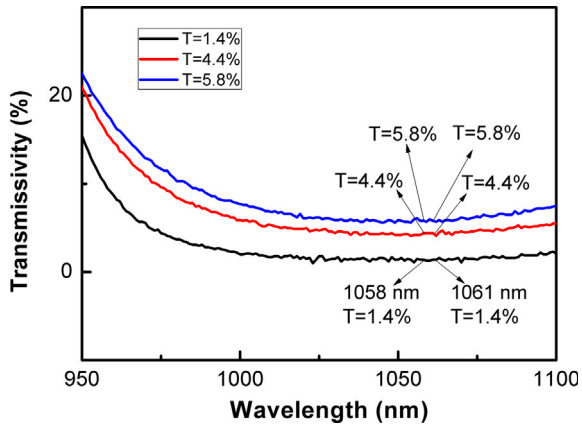

Fig. 2. The transmittance of the three OCs from 950 to 1100 nm.

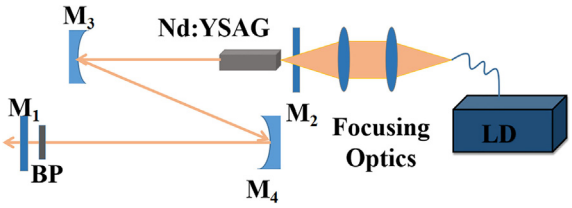

Fig. 3. Experimental setup for QML Nd:YSAG laser.

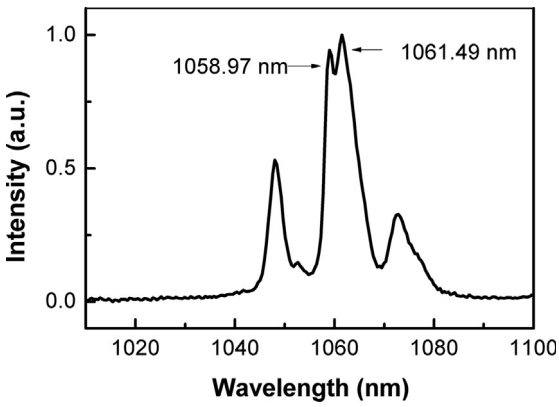

Fig. 4. Fluorescence spectrum of Nd:YSAG crystal.

lasers operate at the dual-wavelengths, and useful for THz generation [13–14]. These optical properties prove that Nd:YSAG is a promising material for solid-state lasers. Till date, spectroscopic characteristics, and laser performance of Nd:YSAG ceramic have been extensively

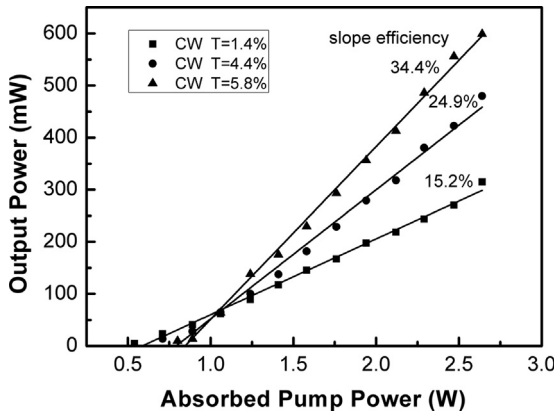

Fig. 5. Output power versus absorbed pump power of continuous-wave laser.

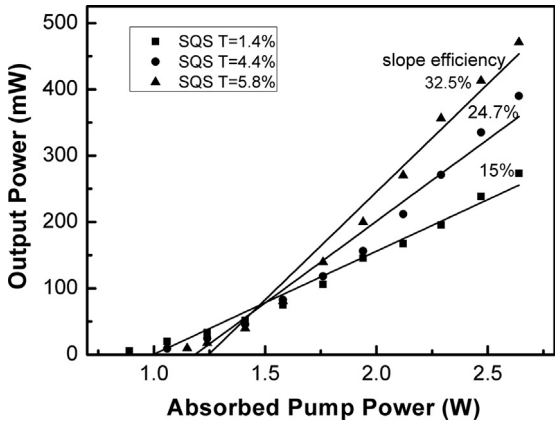

Fig. 6. Output power versus absorbed pump power of self-Q-switched laser.

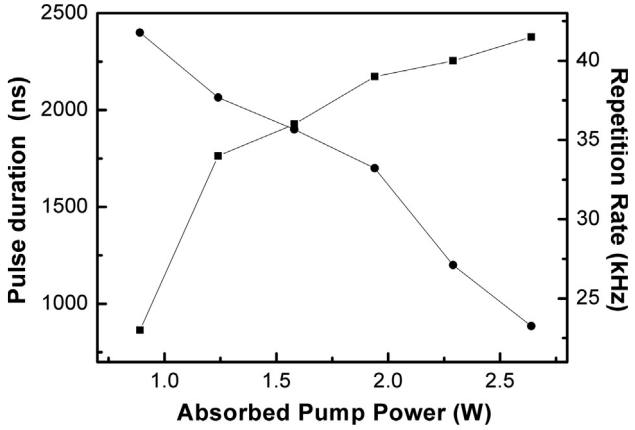

Fig. 7. Pulse duration and repetition rate versus absorbed pump power.

investigated [13–17]. However, the laser performance of Nd:YSAG crystal are rarely reported, only Feng Chao et al. [18] studied the continuous mode-locked Nd:YSAG crystal laser by semiconductor saturable absorber mirror (SESAM). So, laser performance of Nd:YSAG crystal is necessary to study. The performance on self-Q-switching (SQS), and passively Q-switched mode-locking (QML) operation by using black phosphorus (BP) in Nd:YSAG crystal lasers have not been reported.

One of the mechanisms to generate microseconds to nanoseconds is SQS. This technique only needs a pump source, gaining medium, and an optical resonator. The key potential of SQS technique is that there is no need for additional Q-switching element inside the lasing to start and keep the pulsing [19,20]. These characteristics make SQS to be a

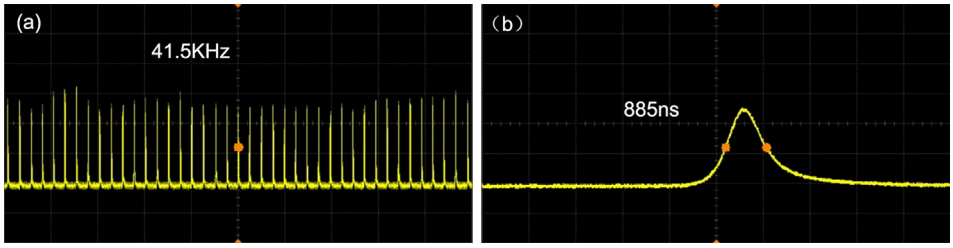

Fig. 8. Typical pulse train and pulse profile of the self-Q-switched laser, (a) 100 μs/div, (b) 1 μs/div.

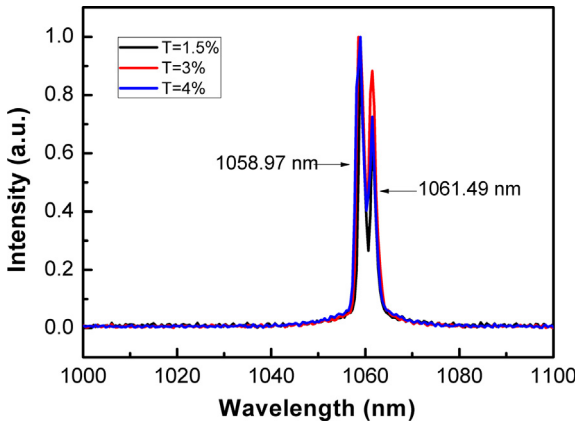

Fig. 9. Spectrum of self-Q-switched laser Nd:YSAG laser.

potential method for generating nanosecond laser pulses. The QML lasers have been also great interest due to high repetition rate and high peak power. In QML operation, saturable absorbers are the core component of the laser. The newly emerging two-dimensional (2D) materials, such as graphene, topological insulators (TIs), Mxene, Transition-metal dichalcogenides (TMDs), and BP [21–24] have shown good performance in generating ultrafast lasers [25]. Graphene has broadband saturable absorption property with an ultrafast recovery time of 200 fs, and a wide operation spectral range covering several micrometers [21]. However, strong light-matter interaction is required due to the absence of band-gap and the low absorption co-efficiency (2.3%/layer). Consequently, it restrains the graphene used to a certain degree. TIs SA has a broadband response wavelength range of saturable absorption, strong saturation intensity, large modulation depth [22]. Nevertheless, complicated preparation process reduces the application in optoelectronic devices. MXene has highly tunable and tailorable electronic/optical properties, but the synthesis process is complex and costly [23]. TMDs have relatively large band gaps, and the optical response occurs mainly in the range of near or visible light [24]. In recent years, BP has attracted much attention. The bandgap of BP strongly depends on the number of layers from 2.0 eV for a single layer to 0.3 for bulk. BP has potential optical applications in the wavelength from 0.6 μm to 4 μm due to its bandgap characteristics [26–28]. The discovery of BP fills the gap between graphene and TMDs. In addition, BP owns a direct bandgap independent of the layer number, which makes it have high absorption and adjustable optical modulation depth [28].

In this paper, dual-wavelength SQS and QML operation of the Nd:YSAG crystal is demonstrated using the BP as a saturable absorber (SA). The dual-wavelengths of 1058.97 and 1061.49 nm are obtained. Material and methods are discussed in Section 2. Section 3 consists of the results and analysis of SQS laser and QML with black phosphorus saturable absorber (BP-SA). Section 4 comprises the conclusion of work.

2. Materials and experiments

2.1. Materials

Isopropyl alcohol, black phosphorus, ethanol, fiber-coupled laser diode, Nd:YSAG crystal, flat mirror M_2 (high reflection, HR = 1060 nm, and high transmission, HT = 808 nm), flat mirror M_1 (transmission, T = 1.4, 4.4, and 5.8% at 1060 nm), M_3 (radius of curvature, R = 400 nm, HR = 1060 nm) and M_4 (R = 200 nm, HR = 1060 nm).

2.2. Self-Q-switching laser

The pump source of a fiber-coupled laser diode (LD) (400 μm in diameter, NA = 0.22) was used with a center wavelength of 808 nm. The experimental setup of the continuous wave (CW) and SQS laser is shown in Fig. 1. In the experiment, a 1:1 focusing system was used to focus the spot to the center of the crystal. The Nd:YSAG crystal was used in the experiment of dimension of $2 \times 2 \times 6\ mm^3$. The crystal was wrapped with indium foil and placed in a water-cooled copper mount at 18 °C. The input coupler (IC) was a flat mirror M_2. This was coated with high reflection (HR), and high transmission (HT). The coating wavelength of the HR and HT were 1060 nm and 808 nm, respectively. Here, M_1 is output coupler (OC). There were three OCs used in the experiments of transmission 1.4, 4.4, and 5.8% at 1058 and 1061 nm wavelength, as shown in Fig. 2.

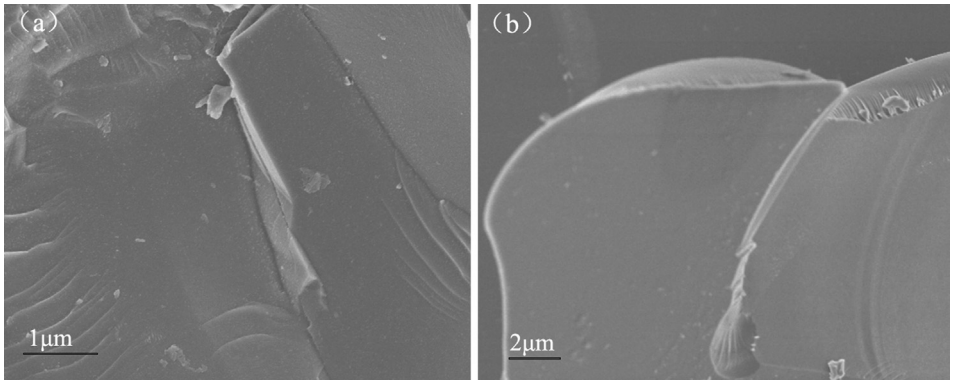

Fig. 10. Scanning electron microscopic images of black phosphorus saturable absorber.

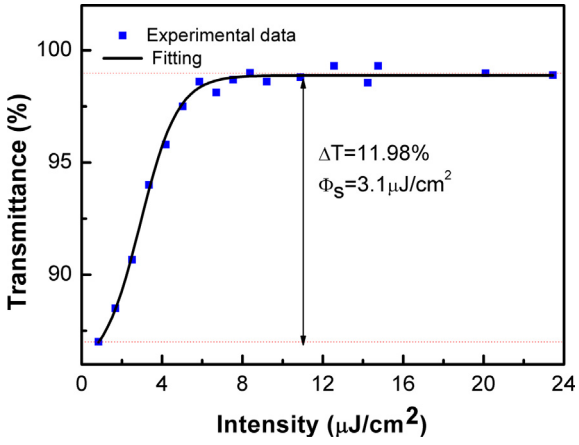

Fig. 11. Nonlinear saturable absorption curve of black phosphorus saturable absorber.

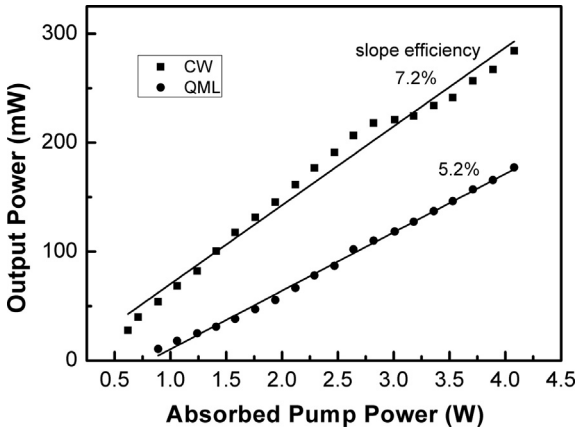

Fig. 12. Continuous-wave and Q-switched mode-locked output power of the Nd:YSAG laser.

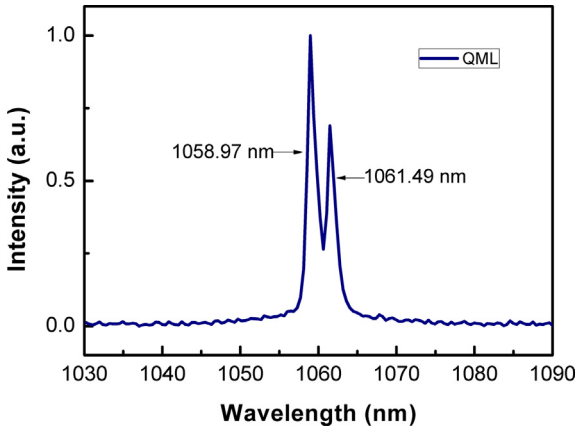

Fig. 13. Spectrum of Q-switched mode-locked Nd:YSAG laser.

2.3. Q-switched mode-locking with black phosphorus saturable absorber

This section presents the validation of an experiment in the presence of QML laser with BP-SA. Firstly, the exfoliated flakes of BP bulk crystal are grinded sufficiently. After that, the BP powder is dispersed in isopropyl alcohol (IPA). The attained solution was ultrasonically stirred for 3 h, and further processed it by centrifugation at the rate of 1500 rpm for 30 min. Afterward, a layer of solution (BP in IPA) was deposited over a glass substrate, and dried in a vacuum oven at room temperature for 12 h. Finally, the substrate was soaked in ethanol, and further sonicated for 5 min to remove the presence of IPA [29]. During ultrasonic and centrifugation in the preparation, the bottle is filled with nitrogen and sealed. After making BP-SA, the outermost layer will form an oxidation film to protect the inner layer of BP. In this way, we can avoid the oxidation issue of BP.

In the experiment, a typical Z-folded resonator cavity was designed to analyze the mode-locking performance of the Nd:YSAG crystal as depicted in Fig. 3. The front part of the experimental device is the same as the SQS. The length of the overall cavity was about 1550 mm for QML Nd:YSAG laser. Here, length from M_2 to M_3 is 220 mm, M_3 to M_4 is 1220 mm, M_4 to BP-SA is 106 mm, and BP to M_1 is 4 mm. M_2 was a flat mirror with HR coated at a wavelength of 1060 nm, and HT was coated at a wavelength of 808 nm. Both M_3 (radius of curvature, R = 400 nm) and M_4 (R = 200 nm) were concave mirrors. These mirrors were also HR coated at 1060 nm. The transmission of the M_1 mirror was 1.4% at 1058 nm laser wavelength.

3. Results and analysis

The fluorescence spectrum of Nd:YSAG crystal is shown in Fig. 4. There are two peaks appears at 1060 nm of similar intensity. These two peaks were divided due to the energy levels splitting of Stark effect.

Firstly, in the CW operation, the cavity mirror was adjusted to the optimum position so that output power reaches the maximum value. We observed the SQS operation by fine-tuning the angle of the output mirror in a repeatable manner. Figs. 5 and 6 shows the output power versus absorbed pump power of the CW and SQS Nd:YSAG lasers with all the OCs 1.4%, 4.4%, and 5.8%. When 1.4% OC is used, the absorbed pump thresholds are 0.54 W and 0.89 W for CW operation and SQS operation, respectively. The output power increases linearly and steadily with the absorption pump power. When the absorbed pump power increased to 2.64 W, the output power reaches to 0.32 W and 0.27 W respectively, and the corresponding slope efficiencies were 15.2% and 15% respectively. When 4.4% OC is used, the absorbed pump thresholds were 0.71 W and 1.06 W for CW operation and SQS operation, respectively. When the absorbed pump power increased to 2.64 W, the output power reaches to 0.48 W and 0.39 W respectively, and the corresponding slope efficiencies were 24.9% and 24.7% respectively. When 5.8% OC is used, the absorbed pump thresholds were 0.8 W and 1.15 W for CW operation and SQS operation, respectively. When the absorbed pump power increased to 2.64 W, the output power reaches 0.6 W and 0.47 W respectively, and the corresponding slope efficiencies were 34.4% and 32.5% respectively. It can be concluded from the above experiments, that the laser pump threshold, maximum output power, and slope efficiencies are increasing with the increase in the transmission.

With the 1.4% OC, we measured the changes in pulse duration and repetition rate by adjusting the pump power. As shown in Fig. 7, the pulse duration decreases with the increase of pump power while the repetition rate increases with the increase of pump power. When the absorbed pump power increases from 0.89 W to 2.64 W, the repetition rate increases from 23 kHz to 41.5 kHz and the pulse width decreases from 2.4 μs to 0.885 μs. The typical SQS pulse train and the pulse profile are shown in Fig. 8(a) and (b), respectively. We obtained the shortest pulse duration and the maximum repetition rate under the absorbed pump power of 2.64 W. The 885 ns was the width of shortest pulse duration with a repetition rate of 41.5 kHz.

The spectrum of SQS Nd:YSAG laser is shown in Fig. 9. Two lines at wavelengths 1058.97 and 1061.49 nm were found from the output spectrum. These wavelengths are identical for different OCs. This is completely consistent with the fluorescence spectrum peak shown in Fig. 2. The central wavelength of the spectrum measured at a different time was the same, and very stable. There is a slight jitter between the two wavelengths in intensity, which attributes to the mode competition.

For solid-state lasers, such as ruby, Tm:YAP, Cr^{3+}:LiSAF, Cr:LiCAF,

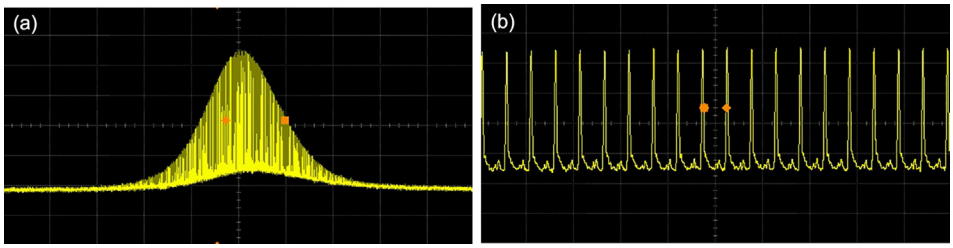

Fig. 14. The Q-switched mode-locked pulse trains measured, (a) 1 μs/div, (b) 20 ns/div.

Nd:GYSGG, and Nd:YVO_4, the SQS operation is due to a non-linear loss mechanism created by a time-dependent lens occurring inside the gain medium and originating from refractive index (RI) changes induced by the population inversion [30–36]. For fiber lasers, such as Tm-doped fiber, the SQS operation is attributed to the reabsorption of the laser photons in the unpumped part of the fiber [37]. In our experiment, the SQS operation is owing to the thermal lens effect in gain medium results in the change of RI and produce the time-dependent lens leads to the non-linear loss mechanism [31,35]. The operation mechanism of SQS operation needs further study.

Fig. 10(a–b) show the scanning electron microscopic (SEM) images of BP-SA, we can clearly see the layered structure of BP-SA. The particles on the surface of BP are residual IPA. The nonlinear absorption of BP-SA was measured by a laser with a wavelength of 1064 nm, a pulse duration of fewer than 15 ps and a repetition rate of 1 MHz. As shown in Fig. 11, the modulation depth and the saturation fluence are 11.98% and 3.1 μJ/cm^2, respectively.

The variation of CW and QML laser in output power regarding the absorbed pump power is shown in Fig. 12. In CW operation, the absorbed pump power threshold was 0.62 W. The maximum average output power of 284.4 mW was obtained with the corresponding slope efficiency of 7.2%, when the absorbed pump power was 4.08 W. Afterward, we insert the BP-SA into the laser cavity and the laser threshold increased from 0.62 W to 0.89 W. A stable QML operation is achieved when the absorbed pump power is increased to 1.41 W. In order to protect crystal and quartz substrate, the maximum absorbed pump power is 4.08 W. The maximum output power of 177.3 mW was obtained under the absorbed pump power of 4.08 W, the corresponding slope efficiency of 5.2%. During the experiment, no optical damage or degradation was observed during the measurements and experiments, even at the highest available optical intensity. Consequently, it is worthy to confirm that the optical damage threshold of the BP-SA is higher than 127.3 μJ/cm^2 (the maximum energy intensity on BP-SA during the experiment). Unfortunately, the exact value of the maximum damage threshold could not be measured under present experimental conditions.

The laser output spectrum for the QML Nd:YSAG laser is shown in Fig. 13. Throughout the whole experiment, working wavelength of QML laser was 1058.97 and 1061.49 nm, which is exactly consistent with the wavelength obtained by SQS.

The Q-switched pulse envelope, and pulse train of the QML Nd:YSAG laser pulse are shown in Fig. 14(a) and (b), respectively. The pulse repetition rate of the mode-locked laser inside the Q-switched envelope is about 96.7 MHz. The QML pulse duration can be estimated by the formula (1) [38]:

$$t_{real}^2 = t_{measure}^2 - t_{probe}^2 - t_{oscilloscope}^2 \quad (1)$$

Here, t_{real} and t_{measure} are the real rise time and measured rise time of the pulse, respectively. t_{probe} and $t_{\mathrm{oscilloscope}}$ are the rise time of the photodiode detector and oscilloscope, respectively. In these experiments, the t_{measure} is about 0.584 ns, the $t_{\mathrm{oscilloscope}}$ and t_{probe} are 0.35 ns and 0.175 ns, respectively. The pulse duration is generally 1.25 times the rising edge. The estimated pulse duration of the mode-locked pulse is about 235 ps.

4. Conclusion

In summarizing, we have studied SQS and QML 1060 nm dual-wavelength of Nd:YSAG lasers. For SQS operation, under the absorbed pump power of 2.64 W, a maximum output power of 471 mW was attained. Besides, we obtained the shortest pulse duration of 885 ns. In the QML state, the pulse duration was calculated to be 235 ps with 96.5 MHz repetition rate under the absorbed pump power of 4.08 W. Both SQS and QML has the same spectrum, operating at two wavelengths. The two wavelengths are 1058.97 and 1061.49 nm, respectively. The results also indicated that Nd:YSAG has potential applications for generating THz, optical communication, and pump-probe measurement.

Acknowledgments

Construction Project Fund for Shandong Province Taishan Mountain Scholars; National Natural Science Foundation of China (NSFC) (61675192); National Key R&D Program of China (2016YFB0402105).

References

[1] G.Q. Hu, et al., Measurement of absolute frequency of continuous-wave terahertz radiation in real time using a free-running, dual-wavelength mode-locked, erbium-doped fibre laser, Sci. Rep. 7 (2007) 42082.
[2] Z. Zhang, et al., Switchable dual-wavelength cylindrical vector beam generation from a passively mode-locked fiber laser based on carbon nanotubes, IEEE J. Sel. Top. Quant. 24 (3) (2018) 1–6.
[3] H.C. Liang, et al., Flexibly Controlling the Power Ratio of Dual-wavelength SESAM-based Mode-locked Lasers with Wedged-bonded Nd:YVO_4/Nd:$GdVO_4$ Crystals, IEEE J. Sel. Top. Quant.. Electron. 24 (5) (2018) 1600605.
[4] R. Gaulton, et al., The potential of dual-wavelength laser scanning for estimating vegetation moisture content, Remote Sens. Environ. 132 (2013) 32–39.
[5] H.T. Huang, et al., V^{3+}:YAG as the saturable absorber for a diode-pumped quasi-three-level dual-wavelength Nd:GGG laser, Opt. Exp. 18 (4) (2010) 3352–3357.
[6] B. Wu, et al., Compact dual-wavelength Nd:$GdVO_4$ laser working at 1063 and 1065 nm, Opt. Exp. 17 (8) (2009) 6004–6009.
[7] S.J. Zhou, et al., Continuous wave dual-wavelength Nd:YVO_4 laser working at 1064 and 1066 nm, Chin. Opt. Lett. 15 (7) (2017) 46–50.
[8] L.J. Chen, et al., Dual-wavelength Nd:YAG crystal laser at 1074 and 1112 nm, Opt. Lett. 36 (13) (2011) 2554–2556.
[9] J. Zhang, et al., Investigations on continuous-wave and passively Q-switched Nd:LuAG ceramic lasers at eye-safe wavelengths, Opt. Mater. 73 (2017) 675–679.
[10] D. Sauder, A. Minassian, M.J. Damzen, High efficiency laser operation of 2 at.% doped crystalline Nd:YAG in a bounce geometry, Opt. Exp. 14 (3) (2006) 1079–1085.
[11] G.B. Lutts, et al., GSAG and YSAG: a study on isomorphism and crystal growth, Opt. Quant. Electron. 22 (1) (1990) S269–S281.
[12] L. Jaffres, et al., Gain structuration in dual-wavelength Nd:YSAG ceramic lasers, Opt. Express. 20 (23) (2012) 25596–25602.
[13] J. Saikawa, et al., Passively mode-locked Nd^{3+}-doped $Y_3ScAl_4O_{12}$ ceramic laser with a cascaded quadratic nonlinear mirror, Osa Trends Opt Photon. Series 319 (2004).
[14] H. Cai, et al., Dual-wavelength competitive output in Nd:$Y_3Sc_{1.5}Al_{3.5}O_{12}$ ceramic disk laser, Opt. Commun. 281 (17) (2008) 4401–4405.
[15] J. Carreaud, et al., Wavelength switching in Nd:YSAG ceramic laser induced by thermal effect Wavelength switching in Nd:YSAG ceramic laser, Laser Phys. Lett. 9 (5) (2012) 344–349.
[16] W.C. Lu, et al., Spectral and laser properties of Nd:YSAG single crystal, Acta Phys. Sin. 66 (15) (2017) 154204.
[17] J. Carreaud, et al., From elaboration to laser properties of transparent polycrystalline Nd-doped $Y_3Al_5O_{12}$ and $Y_3ScAl_4O_{12}$ ceramics: a comparative study, Opt. Mater. 35 (4) (2013) 704–711.
[18] C. Feng, et al., Dual-wavelength synchronously mode-locked laser of a

Nd:$Y_3ScAl_4O_{12}$ disordered crystal, Laser Phys. Lett. 14 (4) (2017) 045804.
[19] P.K. Gupta, et al., Note: Self Q-switched Nd:YVO_4 laser at 914 nm, Rev. Sci. Instrum. 83 (4) (2012) 809.
[20] B. Zhang, et al., Compact self-Q-switched Tm:YLF laser at 1.91 μm, Opt. Laser Technol. 100 (2018) 103–108.
[21] Z.T. Wang, et al., Switchable dual-wavelength synchronously Q-switched erbium-doped fiber laser based on graphene saturable absorber, IEEE Photon. J. 4 (3) (2012) 869–876.
[22] Y. Chen, et al., Large energy, wavelength widely tunable, topological insulator Q-switched erbium-doped fiber laser, IEEE J. Sel. Top. Quant. 20 (5) (2014) 0900508.
[23] X.T. Jiang, et al., Broadband nonlinear photonics in few-layer MXene Ti_3C2T_x (T = F, O, or OH), Laser Photon. Rev. 12 (2) (2018) 1700229.
[24] K. Wang, et al., Ultrafast saturable absorption of two-dimensional MoS_2 nanosheets, ACS Nano 7 (10) (2013) 9260.
[25] L.M. Zhao, et al., Dissipative soliton generation in Yb-fiber laser with an invisible intracavity bandpass filter, Opt. Lett. 35 (16) (2010) 2756.
[26] J. Ma, et al., Few-layer black phosphorus based saturable absorber mirror for pulsed solid-state lasers, Opt. Exp. 23 (17) (2015) 22643–22648.
[27] L.C. Kong, et al., Black phosphorus as broadband saturable absorber for pulsed lasers from 1 μm to 2.7 μm wavelength, Laser Phys. Lett. 13 (2016) 045801.
[28] X.C. Su, et al., Femtosecond solid-state laser based on a few-layered black phosphorus saturable absorber, Opt Lett. 41 (9) (2016) 1945.
[29] X.L. Sun, et al., Passively mode-locked 1.34 μm bulk laser based on few-layer black phosphorus saturable absorber, Opt. Exp. 25 (17) (2017) 20025–20032.
[30] I. Freund, et al., Self-Q-switching in ruby lasers, Appl. Phys. Lett. 12 (1968) 388.
[31] W. Cai, et al., Compact self-Q-switched laser near 2 μm, Opt. Commun. 334 (2015) 287–289.
[32] N. Passilly, et al., Experimental and theoretical investigation of a rapidly varying nonlinear lensing effect observed in a Cr^{3+}:LiSAF laser, J. Opt. Soc. Am. B. 21 (2004) 531–538.
[33] B.C. Weber, et al., Efficient single-pulse emission with submicrosecond duration from a Cr:LiSAF laser, Opt. Commun. 128 (1996) 158–165.
[34] E. Beyatli, et al., Self-Q-switched Cr:LiCAF laser, J. Opt. Soc. Am. B. 30 (2013) 914–920.
[35] Q. Song, et al., Dual-wavelength self-Q-switched Nd:GYSGG laser, T. Mod. Optic. 62 (19) (2015) 1–5.
[36] R.S. Conroy, et al., Self-Q-switched Nd:YVO4 microchip lasers, Opt. Lett. 23 (6) (1998) 457.
[37] A.F. El-Sherif, et al., Dynamics and self-pulsing effects in Tm3+-doped silica fibre lasers, Opt. Commun. 208 (4) (2002) 381–389.
[38] F.Q. Liu, et al., Passively Q-switched mode-locking in a diode-pumped c-cut Nd:$LuVO_4$ laser with Cr^{4+}:YAG, Laser Phys. Lett. 6 (8) (2010) 567–570.